

Complementary Features of Attention Bias Modification Therapy and Cognitive-Behavioral Therapy in Pediatric Anxiety Disorders

Lauren K. White, Ph.D., Stefanie Sequeira, B.S., Jennifer C. Britton, Ph.D., Melissa A. Brotman, Ph.D., Andrea L. Gold, Ph.D., Erin Berman, Ph.D., Kenneth Towbin, M.D., Rany Abend, Ph.D., Nathan A. Fox, Ph.D., Yair Bar-Haim, Ph.D., Ellen Leibenluft, M.D., Daniel S. Pine, M.D.

Objective: In the treatment of anxiety disorders, attention bias modification therapy (ABMT) and cognitive-behavioral therapy (CBT) may have complementary effects by targeting different aspects of perturbed threat responses and behaviors. ABMT may target rapid, implicit threat reactions, whereas CBT may target slowly deployed threat responses. The authors used amygdala-based connectivity during a threat-attention task and a randomized controlled trial design to evaluate potential complementary features of these treatments in pediatric anxiety disorders.

Method: Prior to treatment, youths (8–17 years old) with anxiety disorders (N=54), as well as healthy comparison youths (N=51), performed a threat-attention task during functional MRI acquisition. Task-related amygdala-based functional connectivity was assessed. Patients with and without imaging data (N=85) were then randomly assigned to receive CBT paired with either active or placebo ABMT. Clinical response was evaluated, and pretreatment amygdala-based connectivity profiles were compared among patients with varying levels of clinical response.

Results: Compared with the CBT plus placebo ABMT group, the CBT plus active ABMT group exhibited less severe anxiety after treatment. The patient and healthy comparison groups differed in amygdala-insula connectivity during the threat-attention task. Patients whose connectivity profiles were most different from those of the healthy comparison group exhibited the poorest response to treatment, particularly those who received CBT plus placebo ABMT.

Conclusions: The study provides evidence of enhanced clinical effects for patients receiving active ABMT. Moreover, ABMT appears to be most effective for patients with abnormal amygdala-insula connectivity. ABMT may target specific threat processes associated with dysfunctional amygdala-insula connectivity that are not targeted by CBT alone. This may explain the observation of enhanced clinical response to CBT plus active ABMT.

AJP in Advance (doi: 10.1176/appi.ajp.2017.16070847)

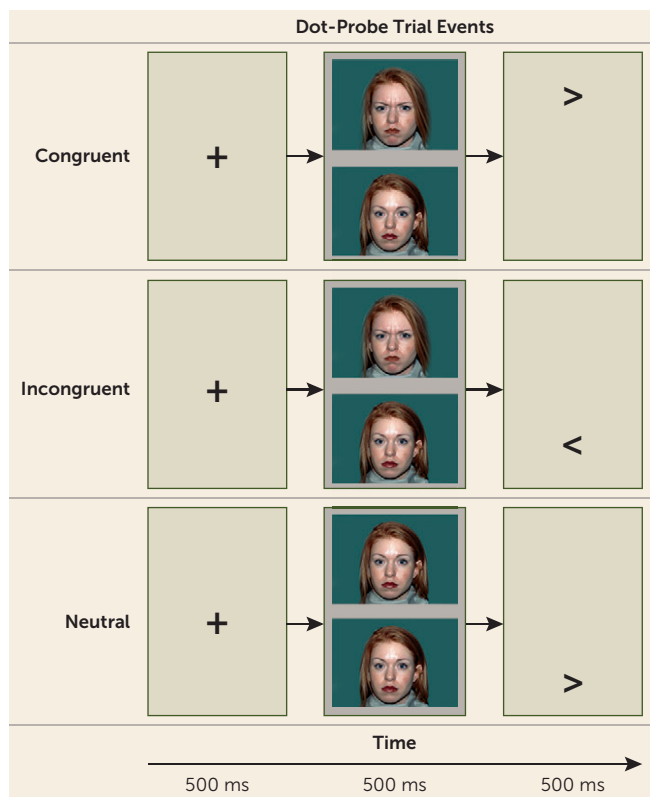
In the treatment of anxiety disorders, attention bias modification therapy (ABMT) and cognitive-behavioral therapy (CBT) may target different aspects of dysfunctional threat processing. In this study, we compared clinical response to active and placebo forms of ABMT in patients receiving CBT. We also differentiated patients with varying clinical response to these treatments by assessing amygdala connectivity engaged during threat-related attention shifts. To do so, we used the dot-probe task and functional MRI (fMRI) in these patients and a group of matched healthy volunteers.

Threats influence attention more strongly in anxious than nonanxious individuals (1). Such effects manifest on paradigms such as the dot-probe task (e.g., 2, 3), which briefly presents task-irrelevant threats. This suggests that anxiety disorders involve implicit biases in attention, and ABMT was developed to alter these attention biases (4–7). ABMT adapts the dot-probe

task to use implicit training to correct these biases by varying the location of task-relevant targets and task-irrelevant threats (Figure 1). In CBT, by contrast, patients learn how to change their attention and behavior through explicit instruction and practice, without receiving the repetitive, implicit training contained in ABMT. Therefore, ABMT could augment clinical response by altering components of implicit biases not fully alleviated by CBT. This may explain why some patients fail to benefit fully from CBT (8).

The different techniques used in CBT and ABMT are reflected in a recently proposed “two-system” model contrasting neural processes engaged by threats (9). The model labels one set of processes “defensive reactions,” which involve rapid, stereotyped behaviors triggered by threats, and contrasts these with a second set, “defensive responses,” which involve more flexible, slowly deployed behaviors. From the

FIGURE 1. The Dot-Probe Task



perspective of this model, ABMT could target defensive reactions in ways that CBT does less directly. By comprehensively changing both sets of processes, CBT with ABMT may produce a greater clinical response than CBT alone or CBT with inactive ABMT. In the present study, we evaluated this possibility through a randomized controlled trial.

Combining a randomized controlled trial with an fMRI assessment of attention biases could identify factors associated with varying levels of clinical response. Such research is particularly needed in youths, where few therapies have been shown to enhance CBT response and few factors have been shown to differentiate youths with poor response to CBT (e.g., 10–13). To characterize patients who manifest varying levels of treatment response, we used fMRI to assess amygdala-based functional connectivity during a dot-probe task. We acquired these data prior to randomly assigning patients receiving CBT to receive, in addition, either an active or a placebo form of ABMT.

Imaging work using the dot-probe task to study anxious individuals has found consistent relationships between anxiety and altered function in circuitry connecting the amygdala to various cortical regions, particularly the insula and the prefrontal cortex (14–16). In the present study, we therefore hypothesized that patients and healthy comparison subjects differ by level of amygdala-insula and amygdala-prefrontal cortex connectivity during the dot-probe task. We also expected that dysfunctional connectivity between the

amygdala and the insula and prefrontal cortex would differentiate patients with particular treatment outcomes, specifically to ABMT.

METHOD

Participants

As in previous National Institute of Mental Health (NIMH) studies, treatment-seeking patients were recruited and matched to healthy comparison subjects in available subject pools (17). All participants had an IQ >70, were medication free, and were assessed by structured interviews (18). Participants had diagnoses of generalized anxiety disorder, social anxiety disorder, and/or separation anxiety disorder. Current major depressive disorder, obsessive-compulsive disorder, and posttraumatic stress disorder were exclusionary, as were a lifetime history of psychosis, bipolar disorder, or extreme trauma. Study procedures were approved by the NIMH institutional review board. Parents and youths provided written consent or assent.

A total of 85 patients were randomly assigned to receive either active ABMT or a placebo version of ABMT, using published methods (19). The protocol under which this study was performed has multiple components, including one with open fluoxetine treatment; for the trial reported here, however, no patient received fluoxetine or any other medication. All personnel working with the patients were blind to ABMT group assignment. Data were collected from the summer of 2012 until the fall of 2015.

Of 85 patients who underwent randomized assignment, two declined participation after randomization, four completed only baseline assessments, and seven could not tolerate CBT; 72 patients completed at least one ABMT session. Of the 58 patients who underwent scanning, MRI data were usable for 54, and of these, 40 had posttreatment clinical assessments (for more information, see the Supplemental Methods section of the data supplement that accompanies the online edition of this article).

Fifty-one healthy youths, group-matched with the patients on age, sex, and IQ (23 of them were female, and the mean age was 12.86 years [SD=1.94]), completed the same preassessment protocol. The patient and healthy comparison groups did not differ significantly in attention bias on the dot-probe task, although reaction time was generally slower in the patient group. Mean reaction time was not related to baseline symptom severity or treatment response (Table 1).

Attention Bias Assessment

Participants completed an event-related dot-probe MRI task (see Figure 1) at baseline (19), with a subgroup undergoing repeat fMRI after treatment. In the dot-probe task, fixation crosses preceded face-pair presentations exhibiting either angry-neutral or neutral-neutral expressions, followed by an arrow probe; participants were instructed to respond to the direction of the probe. The task had three conditions: 1) congruent trials, which presented probes behind the angry

TABLE 1. Demographic and Clinical Characteristics of Youths With Anxiety Disorders and Healthy Comparison Subjects, by Diagnostic Group, for fMRI Analysis

Characteristic or Measure	Anxiety Group (N=54)		Healthy Comparison Group (N=51)	
	N	%	N	%
Female	32	59.3	23	45.1
	Mean	SD	Mean	SD
Age (years)	12.08	2.80	12.86	1.94
IQ	112.78	15.55	113.18	11.58
Baseline SCARED total score ^a	29.40	9.59	5.44	4.68

^a SCARED=Screen for Childhood Anxiety Related Emotional Disorders (total score, averaged across parent and child reports). Significant difference between groups, $p < 0.001$.

face; 2) incongruent trials, which presented probes behind the neutral face; and 3) neutral trials, which lacked angry faces and provided a nonthreat condition. The results highlight the incongruent-congruent contrast, considered a measure of “attention bias” reflecting differential brain function or behavior when attention is allocated away or toward the angry face. The fMRI task was presented across two runs to provide 80 trials of each task condition, interspersed with 80 “null” fixation-only trials. (For more information, see the Supplemental Methods section of the online data supplement.)

Treatments

The flow of participants in the study is illustrated in Figure 2. All patients received up to 12 weekly CBT sessions (see the data supplement) (12, 20); makeup sessions were not available, so patients who missed one or more CBT appointments had fewer than 12 sessions. Patients were randomly assigned to receive active or placebo ABMT, delivered from the fifth through the 12th CBT session. For ABMT, participants received a modified dot-probe task: active ABMT always presented probes in the opposite location of the angry face (incongruent trials); placebo ABMT presented probes with equal probability behind angry or neutral faces (19). Two 5-minute ABMT sessions occurred during each visit, one before and one after the CBT session.

Clinical Treatment Data Analysis

Primary outcome tests followed conventions in the Research Unit on Pediatric Psychopharmacology (RUPP) Anxiety Study (21). To provide the primary continuous clinician-derived index, treating therapists rated the 50-item Pediatric Anxiety Rating Scale (PARS) (22) at pretreatment, midtreatment, and posttreatment assessments. The effects of treatment were examined using the intent-to-treat principle, which included all patients who underwent randomized treatment assignment for whom baseline data and data on any outcome measure were available (N=68). PARS rating data were subjected to a linear mixed model with time (midtreatment, posttreatment assessment) as a within-group variable and ABMT group (active, placebo) as a between-group variable. Data were assumed to

have an autoregressive (AR1) covariance structure. Pretreatment ratings were entered as a covariate. Determination of efficacy was based on the planned contrast that tested ABMT group differences on posttreatment PARS ratings. For the analysis of treatment response as a categorical outcome, determination of efficacy was based on a comparison of clinical response rates on the Clinical Global Impressions improvement (CGI-I) scale, as employed in the RUPP Anxiety Study. Patients who had improvement, defined as having a CGI-I score ≤ 3 , were compared with those with no improvement with the chi-square test. In secondary analyses, models were conducted to test the effects of age and sex on treatment response.

Imaging Data Acquisition and Analysis

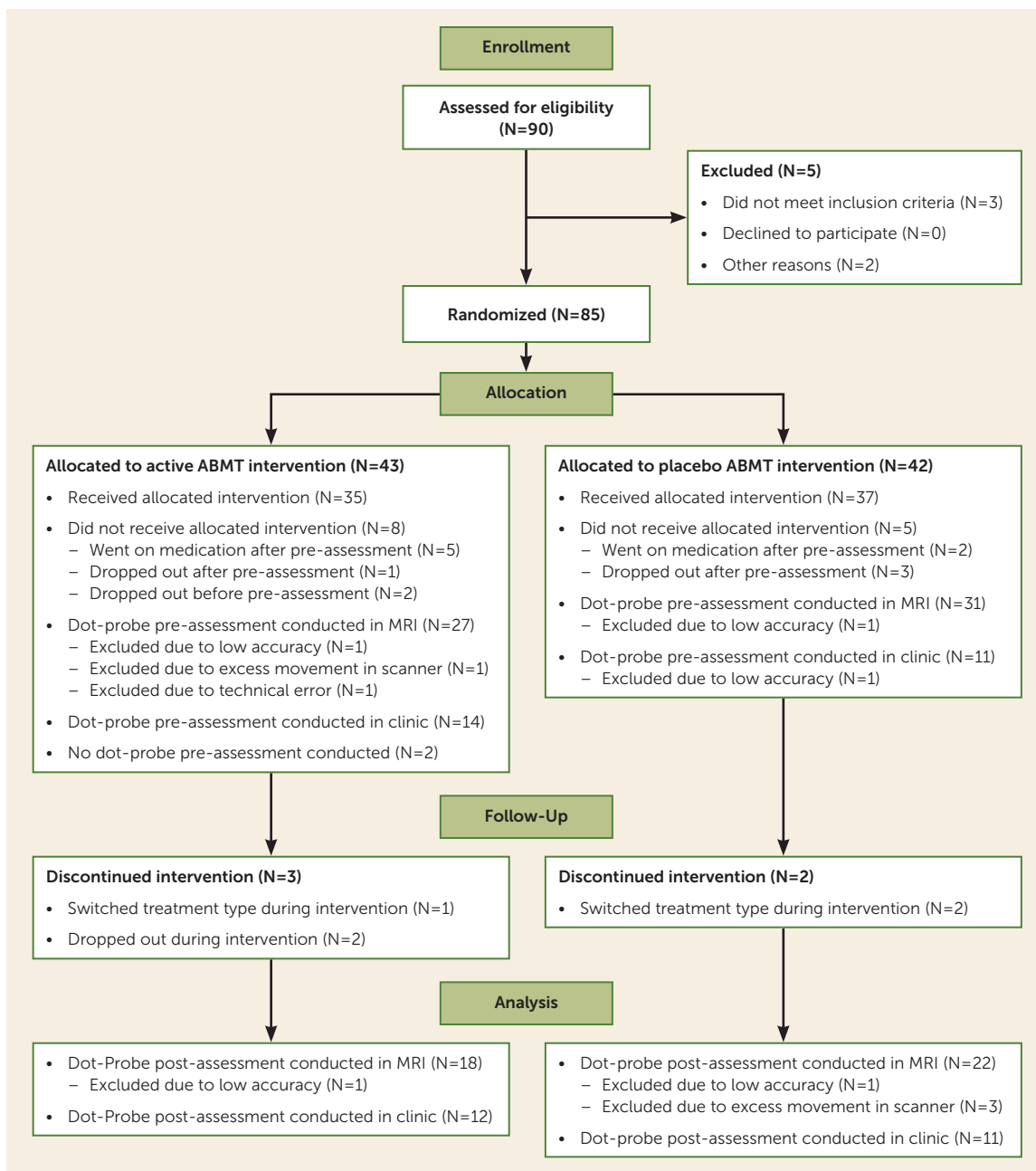
fMRI acquisition parameters. Neuroimaging data were acquired with a 3-T GE scanner (Waukesha, Wisc.) with an eight-channel head coil with $2.5 \times 2.5 \times 2.5$ mm resolution and T_2^* weighting (TR=2,300 ms, TE=25 ms, flip angle=50°, FOV=24 cm, matrix=96×96, 41 contiguous 3-mm interleaved axial slices). Coregistration and normalization used a high-resolution three-dimensional magnetization-prepared rapid gradient echo scan (NEX=1, TE/TI=min/725 ms, FOV=22 cm, matrix=256×192, bandwidth=31.25 Hz per 256 voxels).

fMRI preprocessing. Processing in AFNI (Analysis of Functional Neuroimages) included slice timing correction, coregistration, and normalization and nonlinear registering of echoplanar data to anatomical scans. Data were smoothed (5 mm full width at half maximum) and scaled to 2.5-mm isotropic voxels. For motion correction, repetition time (TR) pairs with a Euclidean norm motion derivative > 1 mm were censored prior to individual-level analyses. To be included in the analyses, no more than 20% of TRs across conditions could be censored.

Individual-level general linear models included regressors for correct trials across task conditions, incorrect trials, and for baseline drift and motion (i.e., rotational movement of roll, pitch, yaw, and motion displacement in the x, y, and z axes). Functional connectivity used generalized psychophysiological interaction (gPPI) to model connectivity between each anatomically defined amygdala in the AFNI Talairach Daemon atlas and other brain regions across each task condition. Separate individual-level general linear models were created for the right and left amygdala seeds. PPI terms for congruent, incongruent, and neutral conditions were the product of detrended and demeaned seed and trial condition regressors. Individual PPI general linear models used the same regressors for task-related changes in activation, in addition to the time series for the seed and the three PPI terms. With gPPI, individual differences in activation are controlled to better isolate task-specific differences in connectivity (23).

fMRI data analysis. All analyses relied on an event-related design and focused on task-related amygdala-based connectivity. This focus reflected the consistency of previous findings

FIGURE 2. Flow Diagram of Patients in a Study of Pediatric Anxiety^a



^aThe diagram includes only the patient group, not the healthy comparison group (N=51).

(14–16) and the greater stability of amygdala-based connectivity than activation on the dot-probe task (24). Thus, the results presented in the main text emphasize omnibus statistical models testing for differences in amygdala-based gPPI functional connectivity across task condition. Other analyses appear in the Supplemental Results section of the online data supplement.

The results are presented in three sections examining how amygdala connectivity at baseline 1) differed between patients and healthy comparison subjects, 2) related to overall treatment response in patients, controlling for ABMT effects, and 3) related to ABMT-specific treatment effects. In the

main text, connectivity findings are highlighted where consistent associations emerged across these three sets of analyses; this convergence occurred only for right amygdala connectivity. Other notable results appear in the data supplement, including between-group comparisons for amygdala activation, associations of age and sex with brain function, treatment-related changes in brain function, and differences in brain function related to clinical indices beyond either diagnosis or PARS treatment response.

Across all analyses, significant clusters were identified using both whole brain and region-of-interest approaches.

With an initial threshold of $p < 0.005$ followed by a gray matter–masked cluster correction, a whole brain cluster threshold of $1,063 \text{ mm}^3$ was needed for a correction of $p < 0.05$. This threshold was determined using 10,000 Monte Carlo simulations in AFNI's 3dClustSim tool with the autocorrelation function correction. Based on findings from previous imaging studies with the dot-probe task, a region-of-interest approach was used to test for significant results specifically in the prefrontal cortex and the insula (14–16, 24). The cluster-wise threshold for the prefrontal cortex was based on a single prefrontal cortex mask, used in a previous study with the dot-probe task (24), that encompassed gray matter voxels anterior to a plane drawn at $y=0$ perpendicular to the anterior commissure–posterior commissure line. Also as in previous studies with the dot-probe task (15), the threshold for the right and left insulae was defined based on the insula Talairach Daemon atlas in AFNI. 3dClustSim produced a cluster-wise threshold size of 734 mm^3 for the prefrontal cortex and 203 mm^3 for each insula, for a correction of $p < 0.05$. The group maps were also thresholded to include only data for which 90% of participants had valid data. All Talairach coordinates are presented in the left-posterior-inferior convention.

Pretreatment amygdala connectivity: The first imaging analyses examined amygdala-based connectivity using individual-level connectivity values (PPI coefficients) for 105 participants (54 patients and 51 healthy comparison subjects). Connectivity values were subjected to a linear mixed-effects model using AFNI's 3dMVM program (25) with baseline group (patients, healthy comparison subjects) as a between-subject variable and task condition (congruent, incongruent, neutral) as the within-subject variable.

Amygdala connectivity and treatment response: The next imaging analyses examined relationships between connectivity and treatment response in 40 patients who had both usable pretreatment dot-probe fMRI data and a posttreatment clinical assessment. This set of analyses also used 3dMVM; posttreatment PARS rating was entered as a continuous variable, ABMT group (active, placebo) as a between-subject variable, and PPI coefficients for task condition (congruent, incongruent, neutral) as the within-subject variable. To control for baseline anxiety, pretreatment PARS rating was entered as a covariate.

Two interactions were tested within one model to yield two sets of results. First, the two-way condition-by-posttreatment PARS interaction was examined in patients as a group; this result maps connectivity related to overall CBT response, controlling for ABMT group and pretreatment PARS rating. Significant interactions were decomposed using partial correlation analyses between connectivity levels and posttreatment PARS rating. The second result considered connectivity related specifically to ABMT treatment response. This result pertained to the three-way condition-by-ABMT-by-posttreatment PARS rating interaction, mapping connectivity uniquely related to treatment differences in either the active or placebo ABMT group relative to the other group. Post

hoc visualization relied on correlations between connectivity levels and posttreatment PARS rating for each of the two ABMT groups. The Fisher r -to- z transformation test was used to test for significant ABMT group differences between correlation coefficient magnitudes.

RESULTS

Clinical Effects of CBT and ABMT

The treatment groups did not differ significantly in demographic characteristics or pretreatment anxiety severity (Table 2). CBT produced marked decreases in anxiety across the two groups ($p < 0.001$), but patients in the active ABMT group had lower posttreatment PARS ratings than patients in the placebo ABMT group, with a medium effect size ($t=2.05$, $df=111.14$, $p=0.043$; Cohen's $d=0.51$) (see Figure 3). There were no significant ABMT group differences on posttreatment CGI-I ratings. There were no interactions with ABMT group and age or sex.

Pretreatment Amygdala Connectivity

The first analysis compared patients and healthy comparison subjects on baseline amygdala connectivity, where no clusters surpassed the whole-brain-corrected threshold. However, a significant right amygdala–right insula cluster surpassed the region-of-interest threshold (cluster size= $1,031 \text{ mm}^3$; peak activation= $41, -6, 14$; $F=8.29$, $df=2, 206$; $p < 0.001$) (Figure 4A). Post hoc tests revealed that the patient and healthy comparison groups did not differ significantly in connectivity on the neutral condition. However, the groups displayed opposite patterns of amygdala–insula connectivity on both the congruent and the incongruent trials (Figure 4B). Thus, on the attention bias contrast (incongruent–congruent), the groups showed a significant difference. The patient group showed greater positive right amygdala–insula connectivity during congruent trials, whereas the healthy comparison group showed greater positive connectivity during incongruent trials.

No findings approached significance for group differences in left amygdala connectivity; however, several significant age-by-diagnosis-by-condition interactions emerged (see Table S1 in the online data supplement). An interaction emerged for connectivity between the left amygdala and the left insula (cluster size= 563 mm^3 ; peak activation= $-32, 13, 1$; $F=12.18$, $df=2, 202$, $p < 0.001$) (see Figure S1A in the data supplement). This interaction reflected distinct associations with age in the patient and healthy comparison groups, as further described in the Supplemental Results section of the data supplement. There were no significant interactions with sex and diagnostic group. Descriptions of between-group differences in amygdala activation, which emerged in the left but not the right amygdala, also appear in the data supplement.

Amygdala Connectivity and Overall Treatment Response

The second analysis, which examined relationships between baseline amygdala-based connectivity and overall treatment

TABLE 2. Demographic Characteristics and Treatment Ratings for Youths With Pediatric Anxiety, by ABMT Group, for Treatment Analysis^a

Characteristic or Measure	Active ABMT Group (N=43)		Placebo ABMT Group (N=42)	
	N	%	N	%
Female	26	60.5	24	57.1
	Mean	SD	Mean	SD
Age (years)	11.62	2.78	11.79	2.73
IQ	110.42	14.66	114.00	15.50
PARS rating				
Pretreatment assessment	17.03	2.56	16.84	3.03
Midtreatment assessment	15.26	3.86	15.38	2.85
Posttreatment assessment ^b	11.97	4.69	13.67	3.25
CGI-I				
Midtreatment assessment	3.86	0.80	4.23	0.69
Posttreatment assessment	3.35	0.88	3.29	0.97

^a ABMT=attention bias modification therapy; PARS=Pediatric Anxiety Rating Scale; CGI-I=Clinical Global Impressions improvement scale.

^b Significant difference between groups, $p < 0.05$.

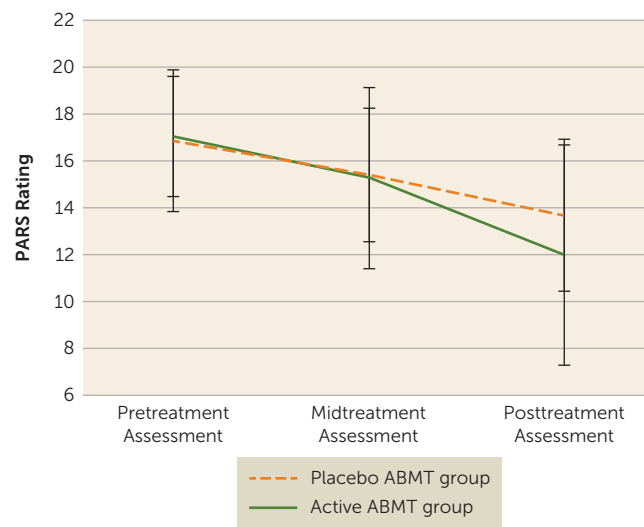
response in patients, revealed several findings that surpassed the whole-brain-corrected threshold (see Table S2 in the data supplement). A significant condition-by-PARS rating interaction was detected for connectivity between the right amygdala and a cluster in the right insula that extended into the superior temporal gyrus (Figure 5A) (cluster size=1,859 mm³; peak activation=54, -24, 9; $F=12.02$, $df=2, 70$, $p < 0.001$). Post hoc correlation analyses showed that the level of baseline amygdala-insula connectivity during congruent trials was positively related to higher posttreatment symptoms on the PARS (Figure 5B). No significant correlation emerged for incongruent trials (Figure 5C). Therefore, on the attention bias contrast (incongruent-congruent), a strongly negative correlation between amygdala-insula connectivity emerged with posttreatment PARS ratings (Figure 5D).

The additional significant findings for right and left amygdala connectivity (see Table S2 in the data supplement) differentiated patients on treatment response; however, they did not differentiate patients from healthy comparison subjects.

Several noteworthy interaction effects emerged with age (see Table S1 in the data supplement). Similar to findings comparing patients with healthy comparison subjects, left amygdala connectivity differed as a function of age and treatment outcome on the PARS in the left insula (see Figure S1B in the data supplement; cluster size=1,391 mm³; peak activation=-51, 11, 11; $F=17.02$, $df=2, 62$, $p < 0.001$). In patients above the median age, the connectivity difference on the attention bias contrast (incongruent-congruent) was negatively associated with posttreatment outcome ratings. This pattern was also seen in patients as a group for the right amygdala, as noted above. There were no significant interactions with sex and overall treatment response.

Amygdala Connectivity and ABMT-Specific Response

The final analysis examined relationships between baseline amygdala connectivity and treatment response as a function of

FIGURE 3. Anxiety Ratings in Youths With Pediatric Anxiety Receiving Cognitive-Behavioral Therapy Plus Active or Placebo Attention Bias Modification Therapy (ABMT)^a

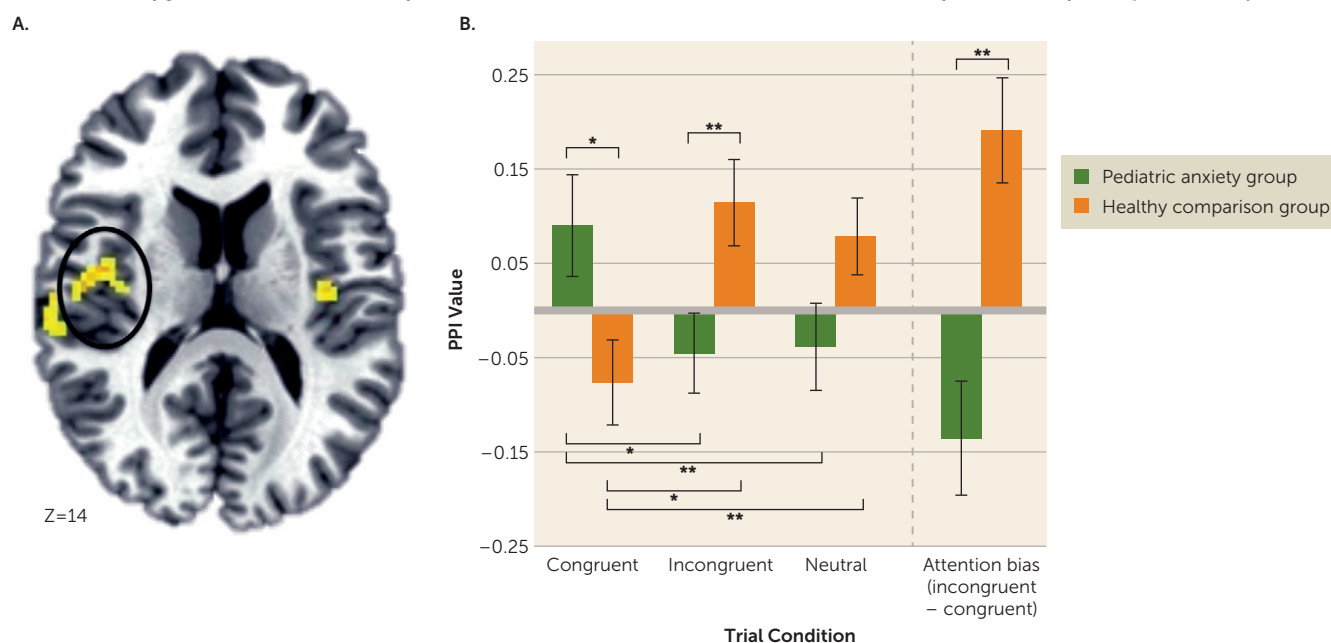
^a PARS=Pediatric Anxiety Rating Scale. Significant difference between groups, $p < 0.05$. Error bars indicate standard deviation.

ABMT group assignment. No findings surpassed the whole-brain-corrected or prefrontal cortex-corrected thresholds. However, there was a significant condition-by-ABMT-by-PARS rating interaction in the right insula extending into the superior temporal gyrus (Figure 6A) (cluster size=516 mm³; peak activation=51, -4, -4; $F=9.57$, $df=2, 70$, $p < 0.001$) that surpassed the insula cluster correction. Correlations between posttreatment PARS rating and connectivity values (Figure 6B-C) revealed no significant relationships within the active ABMT group. However, for patients in the placebo ABMT group, there was a strong relationship between posttreatment symptoms and amygdala-insula connectivity across conditions. Specifically, there was a negative correlation for the attention bias contrast. Moreover, Fisher r -to- z transformation revealed that for the placebo ABMT group, the correlation coefficients for PARS rating and connectivity on congruent ($Z=2.15$, $p=0.03$) and incongruent ($Z=-1.99$, $p=0.05$) conditions were significantly stronger than those observed in the active ABMT group.

No findings approached significance for the condition-by-ABMT-by-PARS rating interaction for the left amygdala seed. Significant interactions with age and sex appear in Table S1 in the data supplement.

DISCUSSION

This study produced three main findings. First, active ABMT enhanced the clinical response to CBT in children and adolescents with anxiety disorders. Second, at study entry, patients differed from healthy comparison subjects in level of amygdala connectivity elicited by an fMRI version of the same task used in ABMT. Third, baseline amygdala functional connectivity differentiated patients' level of treatment

FIGURE 4. Amygdala-Insula Connectivity on a Dot-Probe Task in Youths With Pediatric Anxiety and Healthy Comparison Subjects^a

^a Whole brain random-effects analyses indicated a condition (congruent, incongruent, neutral)-by-anxiety group interaction for connectivity between the right amygdala and insula (panel A; the image is displayed in radiological convention [left=right]; cluster size=1,031 mm³, peak activation=41, -6, 14). Post hoc analyses were conducted (panel B) to examine group differences in connectivity on each task condition as well as on the difference between the incongruent and congruent conditions (i.e., attention bias contrast). PPI=psychophysiological interaction. Error bars indicate standard error. * $p \leq 0.05$. ** $p \leq 0.01$.

response. Some indirect evidence also suggests that active ABMT may correct aspects of perturbed amygdala-based connectivity not targeted by placebo ABMT. These aspects reflect a tendency in patients entering the study to exhibit dysfunctional amygdala-insula connectivity.

ABMT Augmentation of Clinical Response

In this study, we tested whether ABMT augments clinical response to CBT in pediatric anxiety disorders, a question that has been addressed previously in only two randomized controlled trials (5, 26). Augmentation could occur if ABMT targets implicit components of perturbed threat processing that are less directly targeted by CBT (5), reflecting the heterogeneous nature of threat responding (9). We found lower clinician-rated anxiety in patients receiving CBT plus active ABMT compared with patients receiving CBT plus placebo ABMT, which differs from findings in the two previous studies comparing different forms of ABMT added to CBT in pediatric anxiety disorders (5, 26). Several methodological factors may explain the differences; for example, one study included a CBT-alone condition, which produced weak effects (5); the other utilized a different form of ABMT than the one we used (26). Moreover, both of those studies possessed limited statistical power because of small sample sizes. In the present study, group differences emerged on the primary continuous outcome measure, with an effect size of 0.51. While not a large effect, it may represent a clinically meaningful one, comparable in magnitude to the effect of adding a selective serotonin reuptake inhibitor to CBT (12). Nevertheless, no

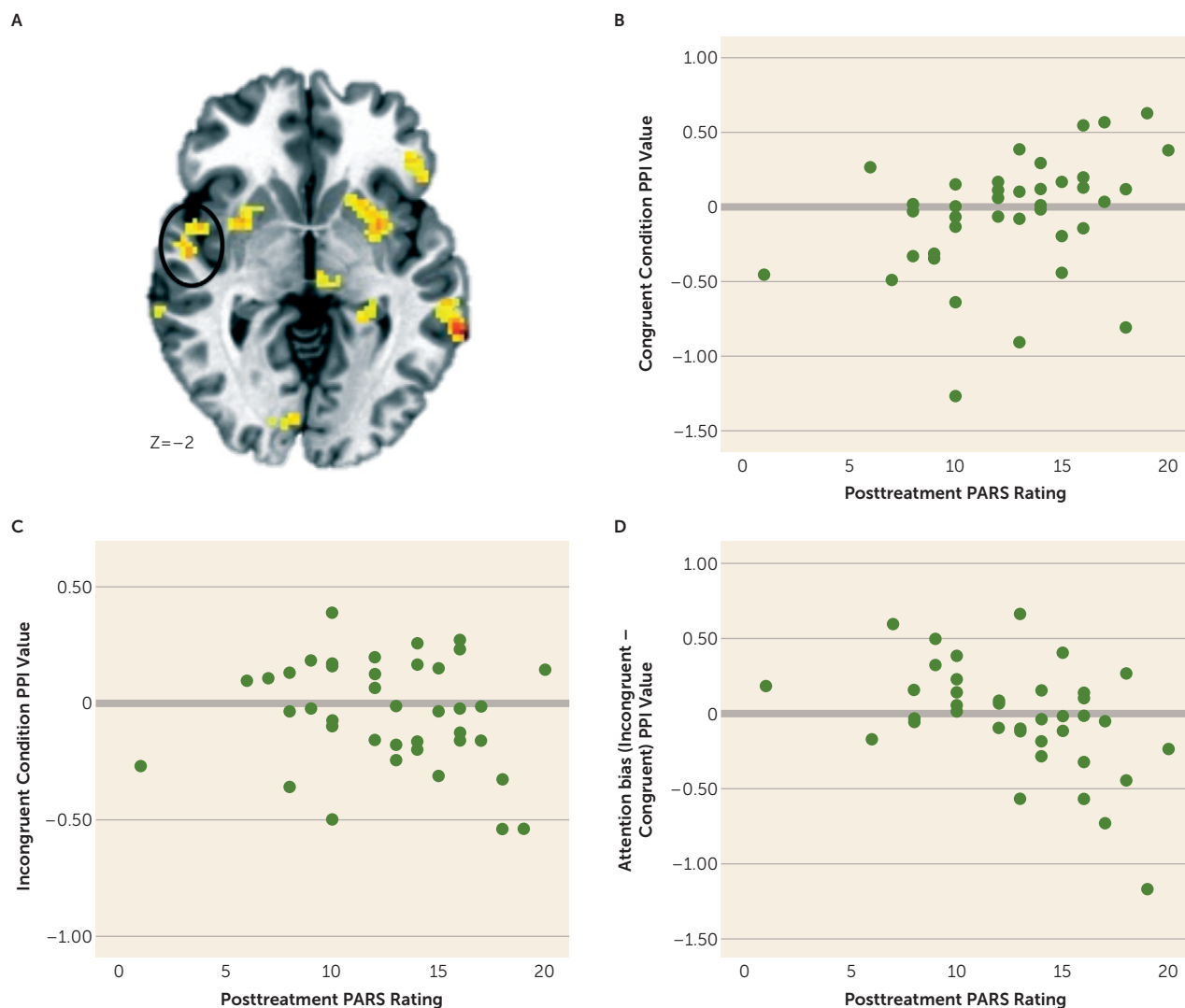
group differences were observed for the categorical outcome measure.

Amygdala-Based Functional Connectivity and Anxiety Disorders

Using imaging data, we also compared healthy subjects and anxiety patients on levels of amygdala connectivity, a measure that has adequate test-retest reliability (24). At study entry, the patient group differed from the healthy group in patterns of functional connectivity between the amygdala and the insula elicited by the dot-probe task, the same task adapted for ABMT.

This finding is similar to findings in other imaging work with the dot-probe paradigm (14–16). In the present study, the patient group differed from the healthy comparison group in both types of angry-face trials, with higher connectivity in the patient group for congruent trials and higher connectivity in the healthy group for incongruent trials. This pattern suggests that youths with anxiety disorders fail to deploy this circuitry effectively when salient, task-irrelevant threats appear as either proximal or distal threats.

Beyond research employing the dot-probe task, previous studies using various imaging techniques have also linked anxiety to perturbed functional amygdala-insula connectivity (27–29). The previous findings suggest that connectivity with the insula allows the amygdala to engage the salience network to deploy attention when threats appear (30, 31). Both imaging and basic research identify the insula, a hub in the salience network, as a region of interest for understanding anxiety and

FIGURE 5. Amygdala-Insula Connectivity on a Dot-Probe Task Related to Overall Treatment Response in Youths With Pediatric Anxiety^a

^a Whole brain random-effects analyses controlling for baseline Pediatric Anxiety Rating Scale (PARS) ratings and attention bias modification therapy (ABMT) indicated a condition (congruent, incongruent, neutral)-by-posttreatment PARS ratings interaction for connectivity between the right amygdala and insula (panel A; the image is displayed in radiological convention [left=right]) (cluster size=1,859 mm³, peak activation=54, 24, 9). To probe the interaction, correlations between posttreatment PARS ratings and condition were examined. Panels B–D are scatterplots between posttreatment PARS rating and congruent ($r=0.43$, $p<0.01$), incongruent ($r=-0.11$, n.s.), and attention bias (incongruent – congruent; $r=-0.48$, $p<0.01$) conditions. PPI=psychophysiological interaction.

threat processing. The insula connectivity findings in this study arose in the mid to posterior insular cortex.

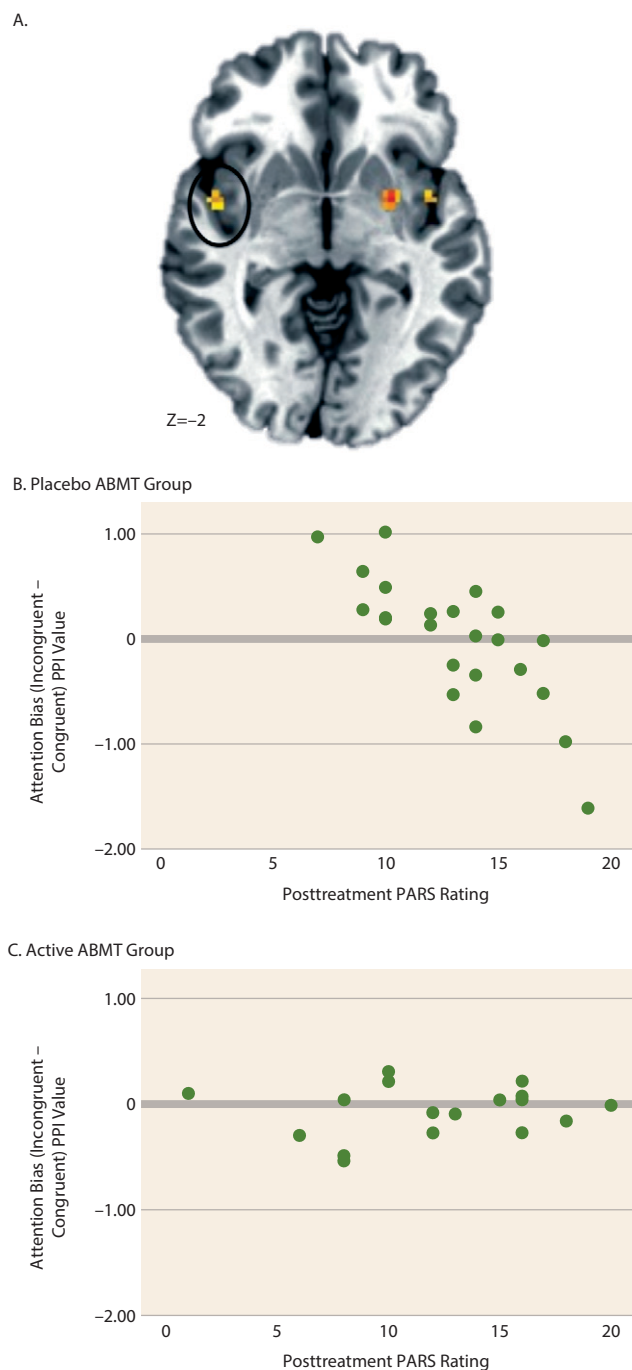
Amygdala-Based Connectivity and Treatment Outcome

We found that amygdala-based functional connectivity was related to both overall and ABMT-specific treatment effects. Overall clinical effects occurred in patients as a group receiving CBT, regardless of ABMT condition. For this first effect, amygdala connectivity in those patients who had an increasingly poor treatment response appeared increasingly different from that of the healthy comparison group. This dysfunctional pattern of amygdala connectivity appeared for the contrast of congruent and incongruent threat trials on the dot-probe task. Thus, at study entry, the patients who

appeared most different from the healthy group on measures of amygdala-insula function exhibited the poorest treatment response.

We also found that patterns of amygdala connectivity differentiated treatment response between the two ABMT groups in a region adjacent to the insula region associated with overall treatment response. Specifically, an association emerged between pretreatment amygdala-insula connectivity and posttreatment anxiety in the group receiving CBT plus placebo ABMT. Of note, no such correlation was seen in the group receiving CBT plus active ABMT. Thus, these preliminary findings suggest that connectivity was related to both the presence of an anxiety disorder and response to a specific type of treatment.

FIGURE 6. Amygdala-Insula Connectivity on a Dot-Probe Task Related to ABMT-Specific Treatment Response in Youths With Pediatric Anxiety^a



^a Whole brain random-effects analyses controlling for baseline Pediatric Anxiety Rating Scale (PARS) ratings indicated an attention bias modification therapy (ABMT) group (active, placebo)-by-condition (congruent, incongruent, neutral)-by-posttreatment PARS ratings interaction for connectivity between the right amygdala and insula (panel A; the image is displayed in radiological convention [left=right]; cluster size=615 mm³, peak activation=45, 0, -4). To probe the interaction, correlations between posttreatment PARS ratings and the attention bias contrast (incongruent - congruent) were examined for each of the ABMT groups. The scatterplots in panels B and C show the association between posttreatment PARS rating and attention bias contrast for the placebo ABMT group ($r=-0.78$, $p<0.001$) and the active ABMT group ($r=0.15$, n.s.). PPI=psychophysiological interaction.

The observed relationships between poor treatment outcome and deficient circuitry functioning in the placebo ABMT group can be understood in the context of the above-mentioned two-process model (9). This pattern could arise if ABMT targets functions associated with perturbed threat reactions that are unaffected by either CBT or placebo ABMT. Such an effect could attenuate the relationship between connectivity at baseline and clinical response after treatment.

Limitations and Conclusions

This study has several limitations. First, the sample size is modest, particularly for the analyses comparing subgroups, such as the fMRI analyses examining ABMT-specific treatment effects. Second, all patients received CBT with either active or placebo ABMT, so our findings may not be generalizable to other effective treatments, such as medication. This design also prevented us from directly comparing ABMT and CBT or isolating key components of the two treatments. A direct comparison would require a design that included both combined treatments and each treatment delivered as a monotherapy. As a result, we could only partially test a two-factor model of anxiety. Third, limitations arise in the analyses that collapse across ABMT conditions because of heterogeneity that is introduced when using a sample of patients who received both forms of ABMT. Fourth, the study found no behavioral group difference in attention bias and thus failed to demonstrate any relevance of disorder in behavior evoked by the dot-probe task. However, the absence of such differences also removes a potential task performance confounder. Lastly, the generalizability of our findings may be affected by the study's exclusionary criteria (e.g., depression, OCD), as well as by the fact that not all participants had usable imaging data.

Despite these limitations, this proof-of-concept study clinically extends a new two-process model (9) regarding treatment complementarity and a new therapeutic modality. Findings generated by adding a brain imaging component to a clinical test of efficacy suggest that ABMT may target processes that are less directly targeted by CBT. Thus, combining ABMT and CBT may produce benefits in youths who might otherwise not fully respond to CBT monotherapy.

In summary, ABMT and CBT may have complementary effects in the treatment of pediatric anxiety disorders. This study produced evidence of enhanced clinical effect for the primary continuous outcome measure, and the clinical effect was related to pretreatment amygdala-insula functional connectivity. Taken together, these clinical and imaging data suggest that ABMT and CBT may target distinct circuitry components, with enhanced clinical effects in combined therapy, possibly arising through influences of ABMT on implicit processes that are less directly targeted by CBT.

AUTHOR AND ARTICLE INFORMATION

From NIMH, Bethesda, Md.; Children's Hospital of Philadelphia, Philadelphia; the Department of Psychology, University of Miami, Coral Gables,

Fla.; the Child Development Laboratory, University of Maryland, College Park; and the Department of Psychology, Tel Aviv University, Tel Aviv.

Address correspondence to Dr. White (lauren.white@nih.gov).

Supported by the NIMH Intramural Research Program.

ClinicalTrials.gov identifier: NCT00018057.

The authors report no financial relationships with commercial interests.

Received July 29, 2016; revisions received Nov. 15, 2016, and Jan. 17, 2017; accepted Feb. 2, 2017.

REFERENCES

- Bar-Haim Y, Lamy D, Pergamin L, et al: Threat-related attentional bias in anxious and nonanxious individuals: a meta-analytic study. *Psychol Bull* 2007; 133:1–24
- Waters AM, Mogg K, Bradley BP, et al: Attentional bias for emotional faces in children with generalized anxiety disorder. *J Am Acad Child Adolesc Psychiatry* 2008; 47:435–442
- Britton JC, Bar-Haim Y, Carver FW, et al: Isolating neural components of threat bias in pediatric anxiety. *J Child Psychol Psychiatry* 2012; 53:678–686
- Pergamin-Hight L, Pine DS, Fox NA, et al: Attention bias modification for youth with social anxiety disorder. *J Child Psychol Psychiatry* 2016; 57:1317–1325
- Shechner T, Rimon-Chakir A, Britton JC, et al: Attention bias modification treatment augmenting effects on cognitive behavioral therapy in children with anxiety: randomized controlled trial. *J Am Acad Child Adolesc Psychiatry* 2014; 53:61–71
- Heeren A, Mogoșe C, Philippot P, et al: Attention bias modification for social anxiety: a systematic review and meta-analysis. *Clin Psychol Rev* 2015; 40:76–90
- Hakamata Y, Lissek S, Bar-Haim Y, et al: Attention bias modification treatment: a meta-analysis toward the establishment of novel treatment for anxiety. *Biol Psychiatry* 2010; 68:982–990
- Mohatt J, Bennett SM, Walkup JT: Treatment of separation, generalized, and social anxiety disorders in youths. *Am J Psychiatry* 2014; 171:741–748
- LeDoux JE, Pine DS: Using neuroscience to help understand fear and anxiety: a two-system framework. *Am J Psychiatry* 2016; 173:1083–1093
- Kujawa A, Swain JE, Hanna GL, et al: Prefrontal reactivity to social signals of threat as a predictor of treatment response in anxious youth. *Neuropsychopharmacology* 2016; 41:1983–1990
- McClure EB, Adler A, Monk CS, et al: fMRI predictors of treatment outcome in pediatric anxiety disorders. *Psychopharmacology (Berl)* 2007; 191:97–105
- Walkup JT, Albano AM, Piacentini J, et al: Cognitive behavioral therapy, sertraline, or a combination in childhood anxiety. *N Engl J Med* 2008; 359:2753–2766
- Compton SN, Peris TS, Almirall D, et al: Predictors and moderators of treatment response in childhood anxiety disorders: results from the CAMS trial. *J Consult Clin Psychol* 2014; 82:212–224
- Monk CS, Telzer EH, Mogg K, et al: Amygdala and ventrolateral prefrontal cortex activation to masked angry faces in children and adolescents with generalized anxiety disorder. *Arch Gen Psychiatry* 2008; 65:568–576
- Hardee JE, Benson BE, Bar-Haim Y, et al: Patterns of neural connectivity during an attention bias task moderate associations between early childhood temperament and internalizing symptoms in young adulthood. *Biol Psychiatry* 2013; 74:273–279
- Price RB, Allen KB, Silk JS, et al: Vigilance in the laboratory predicts avoidance in the real world: a dimensional analysis of neural, behavioral, and ecological momentary data in anxious youth. *Dev Cogn Neurosci* 2016; 19:128–136
- Beesdo K, Lau JYF, Guyer AE, et al: Common and distinct amygdala-function perturbations in depressed vs anxious adolescents. *Arch Gen Psychiatry* 2009; 66:275–285
- Kaufman J, Birmaher B, Brent D, et al: Schedule for Affective Disorders and Schizophrenia for School-Age Children–Present and Lifetime Version (K-SADS-PL): initial reliability and validity data. *J Am Acad Child Adolesc Psychiatry* 1997; 36:980–988
- Abend R, Pine DS, Bar-haim Y: The TAU-NIMH Attention Bias Measurement Toolbox. Tel Aviv, Tel Aviv University, School of Psychological Sciences, Laboratory for Research on Anxiety and Trauma, 2014. <http://people.socsci.tau.ac.il/mu/anxietytrauma/research/>
- Compton SN, Walkup JT, Albano AM, et al: Child/Adolescent Anxiety Multimodal Study (CAMS): rationale, design, and methods. *Child Adolesc Psychiatry Ment Health* 2010; 4:1
- Walkup JT, Labellarte MJ, Riddle MA, et al: Fluvoxamine for the treatment of anxiety disorders in children and adolescents. *N Engl J Med* 2001; 344:1279–1285
- Research Units on Pediatric Psychopharmacology Anxiety Study Group: The Pediatric Anxiety Rating Scale (PARS): development and psychometric properties. *J Am Acad Child Adolesc Psychiatry* 2002; 41:1061–1069
- McLaren DG, Ries ML, Xu G, et al: A generalized form of context-dependent psychophysiological interactions (gPPI): a comparison to standard approaches. *Neuroimage* 2012; 61:1277–1286
- White LK, Britton JC, Sequeira S, et al: Behavioral and neural stability of attention bias to threat in healthy adolescents. *Neuroimage* 2016; 136:84–93
- Chen G, Saad ZS, Britton JC, et al: Linear mixed-effects modeling approach to fMRI group analysis. *Neuroimage* 2013; 73:176–190
- Britton JC, Bar-Haim Y, Clementi MA, et al: Training-associated changes and stability of attention bias in youth: implications for attention bias modification treatment for pediatric anxiety. *Dev Cogn Neurosci* 2013; 4:52–64
- Roy AK, Fudge JL, Kelly C, et al: Intrinsic functional connectivity of amygdala-based networks in adolescent generalized anxiety disorder. *J Am Acad Child Adolesc Psychiatry* 2013; 52:290–299.e2
- Sylvester CM, Corbetta M, Raichle ME, et al: Functional network dysfunction in anxiety and anxiety disorders. *Trends Neurosci* 2012; 35:527–535
- Gold AL, Morey RA, McCarthy G: Amygdala-prefrontal cortex functional connectivity during threat-induced anxiety and goal distraction. *Biol Psychiatry* 2015; 77:394–403
- Uddin LQ: Salience processing and insular cortical function and dysfunction. *Nat Rev Neurosci* 2015; 16:55–61
- Nieuwenhuys R: The insular cortex: a review. *Prog Brain Res* 2012; 195:123–163

SUPPLEMENTAL METHODS

Participants

A total of 58 patients completed the pre-treatment dot-probe task in the magnetic resonance imaging (MRI) scanner. Data from four patients did not meet quality-control criteria (accuracy < 70% n=2; excess movement n=1; technical errors n=1). Twenty-five patients completed a non-fMRI version of the dot-probe task in the clinic prior to treatment. Of the 54 patients with usable pre-assessment fMRI data, 47 had pre-treatment PARS ratings, 45 had mid-treatment PARS ratings, and 40 had post-treatment PARS ratings, and all patients had SCARED data at baseline.

Of the 54 youths assessed with fMRI pre-treatment, 47 were diagnosed with Generalized Anxiety Disorder (GAD) and/or Social Anxiety Disorder (SAD); the seven patients with neither GAD nor SAD had Separation Anxiety Disorder. Other comorbid diagnoses included: Separation Anxiety Disorder (n=18), Specific Phobia (n=21), Attention-Deficit Hyperactivity Disorder (ADHD) (n=9), Selective Mutism (n=3), Tic Disorder (n=2), and Enuresis (n=1).

Of the 54 patients who had baseline fMRI data, 40 completed a post-treatment dot-probe scan. However, data from 5 patients did not meet quality control criteria (accuracy < 70% n=2, excess movement n=3). Twenty-three patients completed the post-treatment dot-probe task in the clinic. Of these 23 patients, three had usable fMRI pre-treatment data for the dot-probe task, and the remaining 20 completed both the pre- and post-treatment dot-probe task in the clinic. A total of 21 patients did not complete a post-treatment dot-probe assessment.

To provide comparison data for the $n=54$ patients with pre-treatment fMRI data, 51 healthy comparisons were selected from a larger pool of $n=62$ subjects to create a sample group-matched with patients on IQ, age, and sex, all $ps >.1$. PARS and CGI-I clinician ratings were not assessed for the healthy comparison group. However, baseline symptoms across patients and healthy comparisons were assessed using parent- and child-completed scales (SCARED)(1); the total scores from parent and child ratings were averaged together to provide a total anxiety score. Among these 51 healthy comparisons, 48 had data on the SCARED collected within 6 weeks of the pre-assessment fMRI scan.

Secondary analyses examined regional neural changes across time associated with treatment. To create a matched healthy comparison data set for the $n=31$ patients with both pre- and post-scan fMRI data, data were assembled from 31 of the 51 healthy comparisons with two dot-probe fMRI assessments, group matched with patients on IQ, age, and sex. Of note, no data reported in the current study from patients appear in prior publications. For the 51 healthy comparisons, some data in a subset of these subjects appear in a prior report on reliability of the dot-probe task (2).

Dot-Probe Pre-processing

On the dot-probe task, RT-based bias scores were calculated using methods from prior research (3,4). For both behavioral and fMRI data, incorrect trials and trials in which RTs were <150 ms or >2000 ms were removed from analyses. Additionally, for each participant, trials with RT >2.5 standard deviations of the mean RT for that condition (Congruent, Incongruent, Neutral) were also removed. RT-based Attention Bias scores were created by subtracting mean RT on Congruent trials from mean RT on Incongruent trials.

Additional Treatment Information

All patients were treated with cognitive behavioral therapy (CBT). CBT treatment followed procedures in the two treatment manuals from the Child and Adolescent Multimodal Study (CAMS), one for patients 13 years-old or younger and the other for patients 14 years-old or older (5,6). Patients were treated by one of two licensed psychologists, both of whom had at least five years of experience using CBT in the treatment of pediatric anxiety disorders. One of these psychologists (EB) had been a supervising CBT therapist in the CAMS study and served as a resource when questions arose about procedures for implementing the CAMS manuals.

Supplemental Data Analyses

The main text highlighted task-based connectivity, specifically the findings that emerged both at baseline for diagnosis and for treatment-related results. The supplement reports on all significant connectivity findings that survived whole-brain correction and corrections for the PFC and insula ROIs. Additionally, the supplemental material reports on significant findings in regional neural activation for the blood-oxygen level dependent response (BOLD). Additionally, ROI analyses that examined task-related differences in baseline amygdala activation between patients and healthy comparisons, as well as in relation to treatment response are reported. These analyses examined differences in the average level of activation in all voxels lying within each of the two anatomically-defined amygdala ROIs.

Finally, a set of three exploratory analyses were examined. First, effects were examined for age and sex on the main interactions of interest. These included baseline brain function differences related to anxiety, overall treatment in patients, and ABMT-specific treatment effects. Second, for both functional connectivity and regional activation, analyses examined

changes in task-based fMRI response before and after treatment in 1) patients and a healthy comparison group and 2) active and placebo AMBT patient groups. To implement the first analysis, pre- and post-treatment imaging data in patients, as well as two scans approximately nine weeks apart in healthy comparisons, were compared using AFNI's 3dLME. Time (Pre, Post) x Condition (Congruent, Incongruent, Neutral) were entered as within subject factors and Group (Patients, Healthy Comparisons) was entered as a between subjects factor. To examine changes across time as a function of ABMT, a similar analysis was conducted within patients, where ABMT Group (Active, Placebo) was substituted as the between subjects factor and PARS ratings were entered as covariates. Third, baseline anxiety differences using a dimensional approach were examined. This fourth set of analyses utilized data in both patients and healthy comparisons, treated as a single group, and examined associations in the combined sample with anxiety using SCARED scores. These analyses utilized data from n=103 participants, as SCARED scores were missing for 2 healthy comparison subjects. These data were subjected AFNI's 3dMVM program with SCARED total scores as a covariate of interest and task condition (Congruent, Incongruent, Neutral) as the within-subject variable. Next, to specifically model associations between specific symptoms of generalized anxiety (GAD) or social anxiety (SAD), similar associations were examined between the two relevant SCARED subscales and brain function. Due to the high correlation ($r = .70$; $p < .001$) between the GAD and SAD subscales and concerns about multi-collinearity, analyses using a single scale (GAD or SAD) are presented

SUPPLEMENTAL RESULTS

Additional findings for pre-treatment anxiety-related differences in amygdala-based connectivity and neural activation

In addition to the significant results reported in the main text, ROI results revealed patients and healthy comparisons also differed in connectivity between the right amygdala and left insula [cluster size = 219 mm³, peak activation = -36, -14, 14]. No findings with left amygdala or regional activation approached significance.

Additional findings for amygdala-based connectivity and neural activation associated with overall treatment response

See Table S2 for a list of all significant clusters. Additional right-amygdala based findings emerged beyond those reported in the main text. Specifically, treatment response was associated with task-based right amygdala connectivity differences in six additional clusters surviving whole brain correction. These included clusters in the PCC/precuneus and bilateral striatum. An additional cluster in the left insula survived the insula ROI threshold. For left amygdala-based connectivity analysis of treatment response, two clusters in the temporal gyrus survived whole brain correction.

The findings with BOLD signals revealed that treatment response was related to differences in regional activation across task conditions in several regions (see Table S2). Clusters in the dorsolateral prefrontal cortex (dlPFC) and left postcentral gyrus survived whole brain correction and a cluster in the right middle frontal gyrus (premotor cortex area) survived the PFC ROI correction.

Additional findings for amygdala-based connectivity and neural activation associated with ABMT-specific treatment response

In addition to the right amygdala–right insula connectivity finding reported in the main text, ABMT-specific response was also associated with right amygdala-left insula connectivity [cluster size = 281mm³, peak activation = -44, -1, -4].

Pre-treatment amygdala activation

The following analyses examined diagnostic differences in baseline amygdala activation on the dot-probe task. Diagnostic differences for activation in the left amygdala, $F(2,206)=3.21$, $p=.042$, reflected a task-related difference in activation for the patient but not the comparison group. Specifically, in patients, amygdala activation was significantly greater in the neutral compared to the incongruent condition, $t(53) = 2.45$ $p=.012$; in the comparison group, amygdala activation did not differ among task conditions. Moreover, post-hoc analyses directly contrasted the two groups also showed a trend for the patient group to manifest greater amygdala activation than the comparison group for both the Congruent and Neutral conditions, $t(104)=1.80$, $p=.07$; $t(104)=1.82$, $p=.07$. Finally, the group-by-condition interaction was not statistically significant for the right amygdala, $F(2,206)=2.84$, $p=.06$. Of note, as reported in the main text, the right amygdala is the location where the main between-group connectivity findings emerged.

Exploratory correlation analyses found no relation between task-related activation in the right ($ps>.10$) or left ($ps>.21$) amygdala at baseline and overall patient treatment outcome. Examining each ABMT group separately, neither the active or placebo groups displayed a significant relation between treatment response and baseline activation in the right ($ps>.13$) or left ($ps>.09$) amygdala.

Additional Exploratory Supplemental Analyses

Age and Sex Effects

The significant interactions with age and sex on the main contrasts of interest are presented in Table S1. As briefly noted in the main text, no age-related findings manifested in the right amygdala. However, left amygdala-left insula connectivity differed among age and diagnostic groups at baseline (see Figure S1a) and predicted treatment outcome. For the baseline findings, in patients, age negatively correlated with connectivity on the Attention Bias contrast (Incongruent - Congruent), $r(54) = -.35$, $p = .009$. For healthy comparisons an opposite pattern emerged: age positively correlated with the Attention Bias connectivity contrast, $r(51) = .30$, $p = .03$.

For the treatment-related left amygdala-left insula finding (see Figure S1b), in adolescent patients, higher symptoms after treatment negatively correlated with connectivity on the Attention Bias contrast, $r(16) = -.64$, $p = .004$ (partial correlation controlling for ABMT group and pre-treatment PARS ratings). No such correlation manifested in the younger patient group, $r(16) = .36$, $p = .14$. Of note, left amygdala-left insula was also significant for the Age X ABMT Group X Condition X Treatment Response interaction; however, given the small sample size the four-way interactions are not interpreted. Similarly, four-way interactions emerged with sex (see Table S1), but are also not interpreted. No other interactions with sex emerged.

Differences in amygdala-based connectivity and neural activation before and after treatment

For the analyses that examined differences in brain function across time, no clusters in either the connectivity or regional activation results surpassed any correction thresholds. This

was true for the analyses that examined differences between patients and healthy comparisons, as well as the analyses that examined differences between patients in the active and placebo ABMT groups.

A dimensional approach to examine pre-treatment anxiety-related differences in amygdala-based connectivity and neural activation

Total SCARED Anxiety Scores. The final set of analyses treated patients and comparison youths as a single group and examined associations with levels of anxiety on the SCARED. For task-based functional connectivity with the right-amygdala seed, whole brain corrected analyses revealed associations in the posterior cingulate cortex (PCC)/precuneus [cluster size = 4141 mm³; peak activation = -1, -64, 29] and medial PFC [cluster size = 1250 mm³; peak activation = 6, 54, -1]. In ROI-based analyses, level of anxiety on the SCARED also correlated with connectivity in the right insula [cluster size = 234 mm³; peak activation = 41, -6, 14] and left insula [cluster size = 234 mm³; peak activation = -34, -14, 16]. No findings emerged with the connectivity for the left amygdala seed or for the regional activation analyses.

Generalized and Social Anxiety Subscales. Using SCARED subscales, GAD but not SAD symptoms predicted connectivity (see Table S3). Many associations were similar to those seen in both the categorical (patients vs. healthy comparisons) and dimensional approaches (total SCARED scores). For example, there was a large association between levels of GAD symptoms and connectivity between the right amygdala and right insula, as detected with the between group analysis focused on diagnostic status and the analysis of the total SCARED scores. There was also strong amygdala-PCC/precuneus connectivity that resembled that detected with SCARED Total Scores and right amygdala-mPFC connectivity survived the PFC threshold

[cluster size = 1000mm³; peak activation = -6, 54, 11]. There was also amygdala-dACC connectivity that survived whole brain correction, a finding that also emerged between patients and healthy comparisons at baseline [cluster size = 813; peak activation = 9, -9, 41], but failed to surpass the ROI threshold (as many voxels fell outside the mask).

Although no associations between GAD symptoms and regional activation emerged, variation in SAD symptoms was related to activation, generating a large cluster encompassing large portions of the amygdala and adjacent structures (Table S3). There was also a second cluster in the amygdala [cluster size = 438 mm³; peak activation = -24, -4, -21], but it did not survive the study's statistical thresholds. In the larger cluster, the high relative to low social anxiety group showed increased activation on the Neutral condition. The high social anxiety group also showed greater activation on Congruent and Neutral trials relative to Incongruent trials.

References

1. Birmaher B, Khetarpal S, Brent DA, Cully M, Balach L, Kaufman J, et al. The Screen for Child Anxiety Related Emotional Disorders (SCARED): scale construction and psychometric characteristics. *J Am Acad Child Adolesc Psychiatry*. 1997;36(4):545–53.
2. White LK, Britton JC, Sequeira S, Ronkin EG, Chen G, Bar-Haim Y, et al. Behavioral and neural stability of attention bias to threat in healthy adolescents. *Neuroimage*. 2016; 136:84–93.
3. Britton JC, Suway JG, Clementi MA, Fox NA, Pine DS, Bar-Haim Y. Neural changes with attention bias modification for anxiety: a randomized trial. *Soc Cogn Affect Neurosci* [Internet]. 2014;in press.
4. Britton JC, Bar-Haim Y, Clementi MA, Sankin LS, Chen G, Shechner T, et al. (2013). Training-associated changes and stability of attention bias in youth: Implications for Attention Bias Modification Treatment for pediatric anxiety. *Developmental Cognitive Neuroscience*. ;4:52–64.
5. Walkup JT, Albano AM, Piacentini J, Birmaher B, Compton SN, Sherrill JT, et al. Cognitive behavioral therapy, sertraline, or a combination in childhood anxiety. *N Engl J Med*. 2008;359(26):2753–66.
6. Compton SN, Walkup JT, Albano AM, Piacentini JC, Birmaher B, Sherrill JT, et al. (2010). Child/Adolescent Anxiety Multimodal Study (CAMS): rationale, design, and methods. *Child Adolesc Psychiatry Ment Health*. 2010;4:1.

TABLE S1. Regions of Differential Amygdala Connectivity and Activation by Age and Sex on the Dot-Probe Task for all Main Analyses

	Peak TLRC Coordinates (LPI)			Cluster Size in mm ³	Location
	x	y	z		
AGE x CONDITION x ANXIETY GROUP					
Neural Activation	-1	23	42	734 ^b	dorsomedial PFC
Functional Connectivity					
<i>Left Amygdala Seed</i>	51	-14	1	1047 ^b	R. Insula/Superior Temporal Gyrus
	46	19	-6	906 ^b	R. ventrolateral PFC
	36	6	41	656 ^b	R. dorsolateral PFC/Premotor Cortex
	-32	13	1	563 ^b	L. Insula
<i>Right Amygdala Seed</i>	-	-	-		<i>no significant clusters</i>
AGE x CONDITION x POST-TREATMENT PARS RATINGS					
Neural Activation	-	-	-		<i>no significant clusters</i>
Functional Connectivity					
<i>Left Amygdala Seed</i>	-51	11	11	1391 ^a	L. Insula/ventrolateral PFC
	31	9	-11	1047 ^b	R. Inferior Frontal Gyrus
	-29	14	16	234 ^b	L. Insula
<i>Right Amygdala Seed</i>	-39	4	16	406 ^b	L. Insula
	46	-21	14	250 ^b	R. Insula
AGE x ABMT GROUP x CONDITION x POST-TREATMENT PARS RATINGS					
Neural Activation	-	-	-		<i>no significant clusters</i>
Functional Connectivity					
<i>Left Amygdala Seed</i>	-11	-44	46	4,063 ^a	L. Posterior Cingulate Cortex/Precuneus
	-16	-61	24	2,641 ^a	L. Precuneus
	-56	-36	31	2,297 ^a	L. Inferior Parietal Lobule
	59	-26	19	1,531 ^a	R. Postcentral Gyrus
	31	9	-14	1,438 ^a	R. Inferior Frontal Gyrus
	59	-36	29	1,422 ^a	R. Inferior Parietal Lobule
	-4	36	14	1,281 ^a	medial PFC/rostral ACC
	44	16	16	1,172 ^a	R. ventrolateral PFC
	-4	14	31	1,078 ^a	L. dorsal ACC
	41	24	21	1,031 ^b	R. dorsolateral PFC
	-44	-9	9	891 ^b	L. Insula

	36	9	1	219 ^b	R. Insula
<i>Right Amygdala Seed</i>	6	41	9	4,953 ^a	medial PFC/rostral ACC
	4	6	-1	1,734 ^a	rostral ACC/Caudate
	-24	24	-6	844 ^b	L. Insula/Inferior Frontal Gyrus
	-31	9	-4	281 ^b	L. Insula
	41	-14	6	234 ^b	R. Insula

SEX x ABMT GROUP x CONDITION x POST-TREATMENT PARS RATINGS

Neural Activation	-18	56	27	1,250 ^a	L. dorsolateral PFC
	-4	36	41	875 ^b	dorsomedial PFC
	-26	31	44	797 ^b	L. dorsolateral PFC
	-31	16	3	781 ^b	L. Insula/Clasutrum
Functional Connectivity					
<i>Left Amygdala Seed</i>	-	-	-		<i>no significant clusters</i>
<i>Right Amygdala Seed</i>	-	-	-		<i>no significant clusters</i>

TLRC = Talairach; ACC= anterior cingulate cortex; PFC = prefrontal cortex; ^a indicates clusters that surpassed the whole brain correction, ^b indicates the findings surpassed the ROI threshold correction (i.e., PFC or Insula); Gender did not interact with any other contrasts of interest

TABLE S2. Regions of Differential Amygdala Connectivity on the Dot-Probe Task that Predict Treatment Response in Anxious Youths

	Peak TLRC Coordinates (LPI)			Cluster Size in mm ³	Location
	x	y	z		
CONDITION x POST-TREATMENT PARS RATINGS					
Neural Activation					
	34	24	41	2,141 ^a	R. dorsolateral PFC
	-34	-34	49	1,172 ^a	L. Postcentral Gyrus
	41	9	51	1,047 ^b	R. Premotor Cortex
Functional Connectivity					
<i>Left Amygdala Seed</i>	-44	-51	21	1,781 ^a	L. Superior Temporal Gyrus
	-61	-44	1	1,656 ^a	L. Middle Temporal Gyrus
<i>Right Amygdala Seed</i>	-1	-69	14	9,203 ^a	L. Posterior Cingulate Cortex
	-29	1	-1	1,906 ^a	L. Striatum/Lentiform Nucleus/Putamen
	54	-24	9	1,859 ^a	R. Insula/Superior Temporal Gyrus
	-49	-14	44	1,578 ^a	L. Postcentral Gyrus
	-41	-54	16	1,438 ^a	L. Superior Temporal Gyrus
	16	-1	54	1,281 ^a	R. Supplemental Motor Area
	21	6	9	1,219 ^a	R. Striatum/Lentiform Nucleus/Putamen
	-51	-19	19	641 ^b	L. Insula/Postcentral Gyrus

TLRC = Talairach; PFC = prefrontal cortex; ^aindicates clusters that surpassed the whole brain correction, ^bindicates the findings surpassed the ROI threshold correction (i.e., PFC or Insula)

TABLE S3. Regions of Differential Amygdala Connectivity and Activation as a Function of Generalized and Social Anxiety During the Dot-Probe Task

	Peak TLRC Coordinates (LPI)			Cluster Size in mm ³	Location
	x	y	z		
CONDITION X GAD SCARED ANXIETY SCORES					
Neural Activation	-	-	-	-	<i>no significant clusters</i>
Functional Connectivity					
<i>Left Amygdala Seed</i>	-	-	-	-	<i>no significant clusters</i>
<i>Right Amygdala Seed</i>	46	6	14	3,016 ^a	R. Insula
	-1	-56	44	2,016 ^a	L. Precuneus
	-41	-71	26	1,406 ^a	L. Middle Temporal Gyrus
	-4	4	36	1,078 ^a	dorsal ACC
	-6	54	11	1,000 ^b	medial PFC
	-34	-14	16	484 ^b	L. Insula
CONDITION X SAD SCARED ANXIETY SCORES					
Neural Activation	1	-16	-14	2,641 ^a	R. Amygdala/ Red Nucleus
Functional Connectivity					
<i>Left Amygdala Seed</i>	-	-	-	-	<i>no significant clusters</i>
<i>Right Amygdala Seed</i>	-	-	-	-	<i>no significant clusters</i>

TLRC = Talairach; GAD = Generalized Anxiety; SAD = Social Anxiety Disorder; ACC= anterior cingulate cortex; PFC = prefrontal cortex; ^a indicates clusters that surpassed the whole brain correction, ^b indicates the findings surpassed the ROI threshold correction (i.e., PFC or Insula)

FIGURE S1. Left amygdala-left insula functional connectivity associated age on the Dot-Probe Task. **a.** Age differences between anxious and healthy comparisons across task condition were detected in connectivity between the left amygdala and left insula [cluster size =563 mm³, peak activation = -32,13,1]. **b.** Treatment analyses also showed age-related effects in left amygdala-left insula connectivity [cluster size= 1391mm³, peak activation= -51,11,11] that emerged from the Condition-by-Age-by-Post-treatment PARS interaction. Images displayed in radiological convention (left-right).

